Wellhead and Surface Gathering Systems

10-1 INTRODUCTION

This chapter is concerned with the transport of fluids from the wellhead to the facility where processing of the fluids begins. For oil production, this facility is typically a two- or three-phase separator; for gas production, the facility may be a gas plant, a compressor station, or simply a transport pipeline; and, for injection wells, the surface transport of interest is from a water treating/pumping facility to the wells. We are not concerned here with pipeline transport over large distances; thus we will not consider the effect of hilly terrain or changes in fluid temperature in our calculations.

As in wellbore flow, we are interested primarily in the pressure as a function of position as fluids move through the wellhead and surface flow lines. In addition to flow through pipes, flows through fittings and chokes are important considerations for surface transport.

10-2 FLOW IN HORIZONTAL PIPES

10-2.1 Single-Phase Flow: Liquid

Single-phase flow in horizontal pipes is described by the same equations as those for single-phase flow in wellbores presented in Chapter 7, but with the simplification that the potential energy pressure drop is zero. If the fluid is incompressible and the pipe diameter is constant, the kinetic energy pressure drop is also zero, and the mechanical energy balance [Eq. (7-15)] simplifies to

$$\Delta p = p_1 - p_2 = \frac{2 f_f \rho u^2 L}{g_c D} \tag{10-1}$$

The friction factor is obtained as in Chapter 7 by the Chen equation [Eq. (7-35)] or the Moody diagram (Fig. 7-7).

EXAMPLE 10-1
Pressure drop in a water injection supply line

The 1000 bbl/d of injection water described in Examples 7-2 and 7-4 is supplied to the wellhead through a 3000-ft-long, 1 1/2-in.-I.D. flow line from a central pumping station. The relative roughness of the galvanized iron pipe is 0.004. If the pressure at the wellhead is 100 psia, what is the pressure at the pumping station, neglecting any pressure drops through valves or other fittings? The water has a specific gravity of 1.05 and a viscosity of 1.2 cp.

Solution Equation (10-1) applies, with the Reynolds number and the friction factor calculated as in Chapter 7. Using Eq. (7-7), the Reynolds number is calculated to be 53,900; from the Chen equation [Eq. (7-35)], the friction factor is 0.0076. Dividing the volumetric flow rate by the pipe cross-sectional area, we find the mean velocity to be 5.3 ft/sec. Then, from Eq. (10-1),

$$\Delta p = p_1 - p_2 = \frac{(2)(0.0076)(65.5\ \text{lb}_m/\text{ft}^3)(5.3\ \text{ft/sec})^2(3000\ \text{ft})}{(32.17\ \text{ft-lb}_m/\text{lb}_{f\text{-sec}^2})[(1.5/12)\ \text{ft}]} \tag{10-2}$$

$$= 20{,}800\ \text{lb}_f/\text{ft}^2 = 145\ \text{psi}$$

so

$$p_1 = p_2 + 145\ \text{psi} = 100\ \text{psi} + 145\ \text{psi} = 245\ \text{psi} \tag{10-3}$$

This is a significant pressure loss over 3000 ft. It can be reduced substantially by using a larger pipe for this water supply, since the frictional pressure drop depends approximately on the pipe diameter to the fifth power. ◇

10-2.2 Single-Phase Flow: Gas

The pressure drop for the horizontal flow of a compressible fluid (gas), neglecting the kinetic energy pressure drop, was given by Eqs. (7-50) and (7-54). This equation was based on using average values of Z, T, and μ for the entire length of pipe being considered. In a high-rate, low-pressure line, the change in kinetic energy may be significant. In this case, for a horizontal line, the mechanical energy balance is

$$\frac{dp}{\rho} + \frac{u\,du}{g_c} + \frac{2f_f u^2\,dL}{g_c D} = 0 \tag{10-4}$$

For a real gas, ρ and u are given by Eqs. (7-44) and (7-45), respectively. The differential form of the kinetic energy term is

$$u\,du = -\left(\frac{4qZT}{\pi D^2}\,\frac{p_{sc}}{T_{sc}}\right)^2 \frac{dp}{p^3} \tag{10-5}$$

Substituting for ρ and $u\,du$ in Eq. (10-4), assuming average values of Z and T over the length of the pipeline, and integrating, we obtain

$$p_1^2 - p_2^2 = \frac{32}{\pi^2}\,\frac{28.97\gamma_g \overline{ZT}}{Rg_c D^4}\left(\frac{p_{sc}q}{T_{sc}}\right)^2\left(\frac{2f_f L}{D} + \ln\frac{p_1}{p_2}\right) \tag{10-6}$$

which for field units is

$$p_1^2 - p_2^2 = (4.195 \times 10^{-6}) \frac{\gamma_g \overline{ZT} q^2}{D^4} \left(\frac{24 f_f L}{D} + \ln \frac{p_1}{p_2} \right) \tag{10-7}$$

where p_1 and p_2 are in psi, T is in °R, q is in MSCF/d, D is in in., and L is in ft. The friction factor is obtained from the Reynolds number and pipe roughness, with the Reynolds number for field units given by Eq. (7-55).

Equation (10-7) is identical to Eq. (7-50) except for the additional $\ln(p_1/p_2)$ term, which accounts for the kinetic energy pressure drop. Equation (10-7) is an implicit equation in p and must be solved iteratively. The equation can be solved first by neglecting the kinetic energy term; then, if $\ln(p_1/p_2)$ is small compared with $24 f_f L/D$, the kinetic energy pressure drop is negligible.

EXAMPLE 10-2

Flow capacity of a low-pressure gas line

Gas production from a low-pressure gas well (wellhead pressure = 100 psia) is to be transported through 1000 ft of a 3-in.-I.D. line ($\epsilon = 0.001$) to a compressor station, where the inlet pressure must be at least 20 psia. The gas has a specific gravity of 0.7, a temperature of 100°F and an average viscosity of 0.012 cp. What is the maximum flow rate possible through this gas line?

Solution We can apply Eq. (10-7), solving for q. We need the Reynolds number to find the friction factor. However, we can begin by assuming that the flow rate, and hence the Reynolds number, is high enough that the flow is fully rough wall turbulent so that the friction factor depends only on the pipe roughness. From the Moody diagram (Fig. 7-7), we find that $f_f = 0.0049$ for high Reynolds number and a relative roughness of 0.001. Then

$$q = \sqrt{\frac{(p_1^2 - p_2^2) D^4}{(4.195 \times 10^{-7}) \gamma_g \overline{ZT} \left[\left(24 f_f L/D \right) + \ln (p_1/p_2) \right]}} \tag{10-8}$$

Assuming $Z = 1$ at these low pressures,

$$q = \sqrt{\frac{(100^2 - 20^2)(3)^4}{(4.195 \times 10^{-7})(0.7)(1)(560) \{[(24)(0.0049)(1000)/3] + \ln(100/20)\}}} \tag{10-9}$$

$$= \sqrt{\frac{4.73 \times 10^9}{39.2 + 1.61}} = 10{,}800 \text{ MSCF/d} \tag{10-10}$$

Checking the Reynolds number using Eq. (7-55),

$$N_{\text{Re}} = \frac{(20.09)(0.7)(10{,}800)}{(3)(0.012)} = 4.2 \times 10^6 \tag{10-11}$$

so the friction factor based on fully rough wall turbulence is correct.

We find that we can transport over 10 MMSCF/d through this line. Notice that even at this high flow rate and with a velocity five times higher at the pipe outlet than at the entrance, the kinetic energy contribution to the overall pressure drop is still small relative to the frictional pressure drop. ◇

10-2.3 Two-Phase Flow

Two-phase flow in horizontal pipes differs markedly from that in vertical pipes; except for the Beggs and Brill correlation (Beggs and Brill, 1973), which can be applied for any flow direction, completely different correlations are used for horizontal flow than for vertical flow. In this section, we first consider flow regimes in horizontal gas-liquid flow, then a few commonly used pressure drop correlations.

Flow regimes. The flow regime does not affect the pressure drop as significantly in horizontal flow as it does in vertical flow, because there is no potential energy contribution to the pressure drop in horizontal flow. However, the flow regime is considered in some pressure drop correlations and can affect production operations in other ways. Most important, the occurrence of slug flow necessitates designing separators or sometimes special pieces of equipment (slug catchers) to handle the large volume of liquid contained in a slug. Particularly in offshore operations, where gas and liquid from subsea completions are transported significant distances to a platform, the possibility of slug flow, and its consequences, must be considered.

Figure 10-1 (Brill and Beggs, 1978) depicts the commonly described flow regimes in horizontal gas-liquid flow. These can be classified as three types of regimes: *segregated* flows, in which the two phases are for the most part separate; *intermittent* flows, in which gas and liquid are alternating; and *distributive* flows, in which one phase is dispersed in the other phase.

Segregated flow is further classified as being stratified smooth, stratified wavy (ripple flow), or annular. Stratified smooth flow consists of liquid flowing along the bottom of the pipe and gas flowing along the top of the pipe, with a smooth interface between the phases. This flow regime occurs at relatively low rates of both phases. At higher gas rates, the interface becomes wavy, and stratified wavy flow results. Annular flow occurs at high gas rates and relatively high liquid rates and consists of an annulus of liquid coating the wall of the pipe and a central core of gas flow, with liquid droplets entrained in the gas.

The intermittent flow regimes are slug flow and plug (also called elongated bubble) flow. Slug flow consists of large liquid slugs alternating with high-velocity bubbles of gas that fill almost the entire pipe. In plug flow, large gas bubbles flow along the top of the pipe, which is otherwise filled with liquid.

Distributive flow regimes described in the literature include bubble, dispersed bubble, mist, and froth flow. The bubble flow regimes differ from those described for vertical flow in that the gas bubbles in a horizontal flow will be concentrated on the upper side of the pipe. Mist flow occurs at high gas rates and low liquid rates and consists of gas with liquid droplets entrained. Mist flow will often be indistinguishable from annular flow, and many flow regime maps use "annular mist" to denote both of these regimes. "Froth flow" is used by some authors to describe the mist or annular mist flow regime.

Flow regimes in horizontal flow are predicted with flow regime maps. One of the first of these, and still one of the most popular, is that of Baker (1953), later modified by Scott (1963), shown in Fig. 10-2. The axes for this plot are G_l/λ and $G_l\lambda\phi/G_g$, where G_l and G_g are the mass fluxes of liquid and gas, respectively (lb_m/hr-ft^2) and the parameters λ

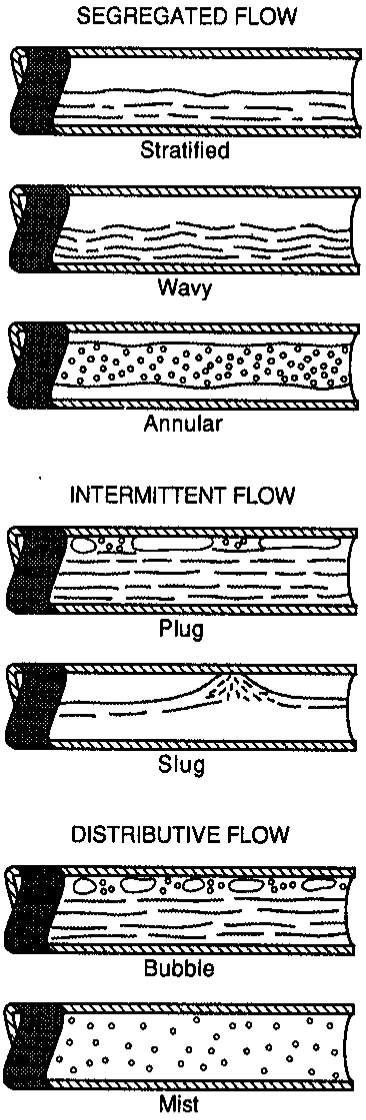

Figure 10-1
Flow regimes in two-phase horizontal flow. (*From Brill and Beggs, 1978.*)

and ϕ are

$$\lambda = \left[\left(\frac{\rho_g}{0.075}\right)\left(\frac{\rho_l}{62.4}\right)\right]^{1/2} \tag{10-12}$$

$$\phi = \frac{73}{\sigma_l}\left[\mu_l\left(\frac{62.4}{\rho_l}\right)^2\right]^{1/3} \tag{10-13}$$

where densities are in lb_m/ft^3, μ is in cp, and σ_l is in dynes/cm. The shaded regions on this

diagram indicate that the transitions from one flow regime to another are not abrupt, but occur over these ranges of flow conditions.

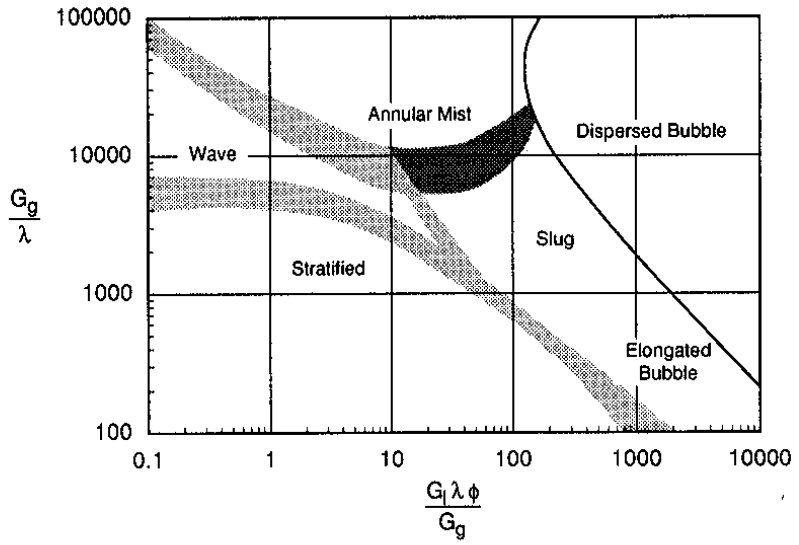

Figure 10-2
Baker flow regime map. (*From Baker, 1953.*)

Another commonly used flow regime is that of Mandhane et al. (1974) (Fig. 10-3). Like many vertical flow regime maps, this map uses the gas and liquid superficial velocities as the coordinates.

The Beggs and Brill correlation is based on a horizontal flow regime map that divides the domain into the three flow regime categories, segregated, intermittent and distributed. This map, shown in Fig. 10-4, plots the mixture Froude number defined as

$$N_{\text{Fr}} = \frac{u_m^2}{gD} \tag{10-14}$$

versus the input liquid fraction, λ_l.

Finally, Taitel and Dukler (1976) developed a theoretical model of the flow regime transitions in horizontal gas-liquid flow; their model can be used to generate flow regime maps for particular fluids and pipe size. Figure 10-5 shows a comparison of their flow regime predictions with those of Mandhane et al. for air-water flow in a 2.5-cm pipe.

EXAMPLE 10-3
Predicting horizontal gas-liquid flow regime

Using the Baker, Mandhane, and Beggs and Brill flow regime maps, determine the flow regime for the flow of 2000 bbl/d of oil and 1 MM SCF/d of gas at 800 psia and 175°F in a 2 1/2-in.-I.D. pipe. The fluids are the same as in Example 7-8.

Solution From Example 7-8, we find the following properties:

Liquid: $\rho = 49.92\ \text{lb}_m/\text{ft}^3$; $\mu_l = 2$ cp; $\sigma_l = 30$ dynes/cm; $q_l = 0.130\ \text{ft}^3/\text{sec}$

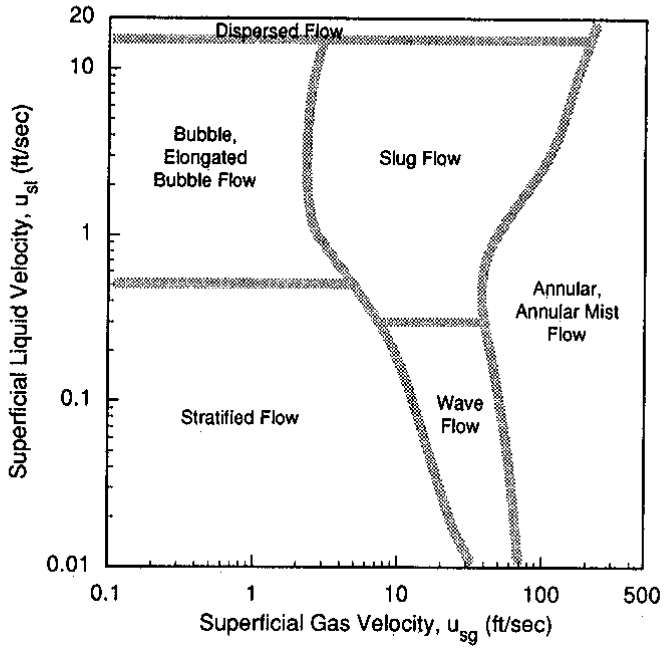

Figure 10-3
Mandhane flow regime map. (*From Mandhane et al., 1974.*)

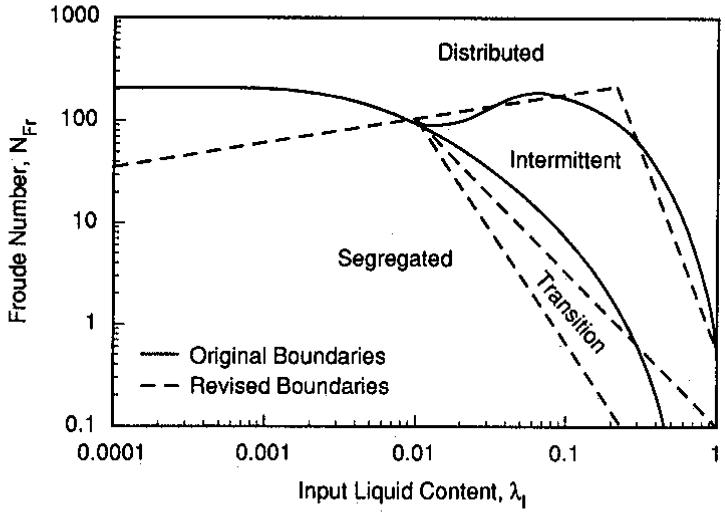

Figure 10-4
Beggs and Brill flow regime map. (*From Beggs and Brill, 1973.*)

Gas: $\rho = 2.6$ lb$_m$/ft^3; $\mu_g = 0.0131$ cp; $Z = 0.935$; $q_g = 0.242$ ft^3/sec

The 2 1/2-in. pipe has a cross-sectional area of 0.0341 ft^2; dividing the volumetric flow rates by the cross-sectional area, we find $u_{sl} = 3.81$ ft/sec, $u_{sg} = 7.11$ ft/sec, and $u_m = 10.9$ ft/sec.

For the Baker map, we compute the mass fluxes, G_l and G_g, and the parameters, λ and

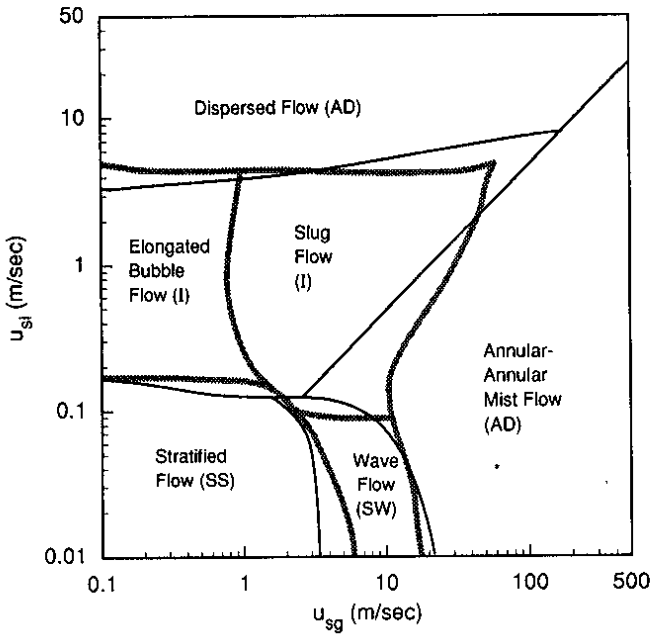

Figure 10-5
Taitel-Dukler flow regime map. (*From Taitel and Dukler, 1976.*)

ϕ. The mass flux is just the superficial velocity times density, so

$$G_l = u_{sl}\rho_l = (3.81 \text{ ft/sec})\left(49.92 \text{ lb}_m/\text{ft}^3\right)(3600 \text{ sec/hr}) = 6.84 \times 10^5 \text{ lb}_m/\text{hr-ft}^2 \quad (10\text{-}15)$$

$$G_g = u_{sg}\rho_g = (7.11 \text{ ft/sec})\left(2.6 \text{ lb}_m/\text{ft}^3\right)(3600 \text{ sec/hr}) = 6.65 \times 10^4 \text{ lb}_m/\text{hr-ft}^2 \quad (10\text{-}16)$$

Then, from Eqs. (10-12) and (10-13),

$$\lambda = \left[\left(\frac{2.6}{0.075}\right)\left(\frac{49.92}{62.4}\right)\right]^{1/2} = 5.27 \quad (10\text{-}17)$$

$$\phi = \frac{73}{30}\left[2\left(\frac{62.4}{49.92}\right)^2\right]^{1/3} = 3.56 \quad (10\text{-}18)$$

The coordinates for the Baker map are

$$\frac{G_g}{\lambda} = \frac{6.65 \times 10^4}{5.27} = 1.26 \times 10^4 \quad (10\text{-}19)$$

$$\frac{G_l\lambda\phi}{G_g} = \frac{(6.84 \times 10^5)(5.27)(3.56)}{6.65 \times 10^4} = 193 \quad (10\text{-}20)$$

Reading from Fig. 10-2, the flow regime is predicted to be dispersed bubble, though the conditions are very near the boundaries with slug flow and annular mist flow.

The Mandhane map (Fig. 10-3) is simply a plot of superficial liquid velocity versus superficial gas velocity. For our values of $u_{sl} = 3.81$ ft/sec and $u_{sg} = 7.11$ ft/sec, the flow regime is predicted to be slug flow.

The Beggs and Brill map plots the mixture Froude number, defined by Eq. (7-125), against the input fraction of liquid. These parameters are

$$N_{\text{Fr}} = \frac{(10.9 \text{ ft/sec})^2}{(32.17 \text{ ft/sec}^2)[(2.5/12) \text{ ft}]} = 17.8 \tag{10-21}$$

$$\lambda_l = \frac{3.81}{10.9} = 0.35 \tag{10-22}$$

From Fig. 10-4, the flow regime is predicted to be intermittent.

The prediction of dispersed bubble flow with the Baker map disagrees with that of Mandhane and Beggs and Brill, which predict slug flow. However, the conditions were very near the flow regime transition on the Baker map, and slug flow is the likely flow regime. ◇

Pressure gradient correlations. Over the years, numerous correlations have been developed to calculate the pressure gradient in horizontal gas-liquid flow. The most commonly used in the oil and gas industry today are those of Beggs and Brill (1973), Eaton et al. (1967), and Dukler (1969). These correlations all include a kinetic energy contribution to the pressure gradient; however, this can be considered negligible unless the gas rate is high and the pressure is low.

Beggs and Brill correlation. The Beggs and Brill correlation presented in Chapter 7 can be applied to horizontal flow, as well as flow in any other direction. For horizontal flow, the correlation is somewhat simplified, since the angle θ is 0, making the factor ψ equal to 1. This correlation is presented in Section 7-4.3, Eqs. (7-125) through (7-152).

EXAMPLE 10-4

Pressure gradient calculation using the Beggs and Brill correlation

Calculate the pressure gradient for the flow of 2000 bbl/d oil and 1 MMSCF/d of gas described in Example 10-3.

Solution The first step in using this correlation is to determine the flow regime using Eqs. (7-131) through (7-134); however, we have already found the flow regime to be intermittent by using the flow regime map in Example 10-3. Note that the dashed lines in Fig. 10-4 correspond to Eqs. (7-131) through (7-134).

Next, we calculate the holdup for horizontal flow with Eq. (7-136). From Example 10-3, $\lambda_l = 0.35$ and $N_{\text{Fr}} = 17.8$, so

$$y_{lo} = \frac{(0.845)(0.35)^{0.5351}}{(17.8)^{0.0173}} = 0.458 \tag{10-23}$$

Even though there is no potential energy contribution to the pressure gradient in horizontal flow, the holdup is used as a parameter in calculating the frictional pressure gradient.

To calculate the frictional gradient, we first obtain the no-slip friction factor based on the mixture Reynolds number. Using Eqs. (7-143), (7-145), and (7-146),

$$\rho_m = (49.92)(0.35) + (2.6)(0.65) = 19.2 \text{ lb}_m/\text{ft}^3 \tag{10-24}$$

The Mandhane map (Fig. 10-3) is simply a plot of superficial liquid velocity versus superficial gas velocity. For our values of $u_{sl} = 3.81$ ft/sec and $u_{sg} = 7.11$ ft/sec, the flow regime is predicted to be slug flow.

The Beggs and Brill map plots the mixture Froude number, defined by Eq. (7-125), against the input fraction of liquid. These parameters are

$$N_{\text{Fr}} = \frac{(10.9 \text{ ft/sec})^2}{(32.17 \text{ ft/sec}^2)[(2.5/12) \text{ ft}]} = 17.8 \tag{10-21}$$

$$\lambda_l = \frac{3.81}{10.9} = 0.35 \tag{10-22}$$

From Fig. 10-4, the flow regime is predicted to be intermittent.

The prediction of dispersed bubble flow with the Baker map disagrees with that of Mandhane and Beggs and Brill, which predict slug flow. However, the conditions were very near the flow regime transition on the Baker map, and slug flow is the likely flow regime. ◇

Pressure gradient correlations. Over the years, numerous correlations have been developed to calculate the pressure gradient in horizontal gas-liquid flow. The most commonly used in the oil and gas industry today are those of Beggs and Brill (1973), Eaton et al. (1967), and Dukler (1969). These correlations all include a kinetic energy contribution to the pressure gradient; however, this can be considered negligible unless the gas rate is high and the pressure is low.

Beggs and Brill correlation. The Beggs and Brill correlation presented in Chapter 7 can be applied to horizontal flow, as well as flow in any other direction. For horizontal flow, the correlation is somewhat simplified, since the angle θ is 0, making the factor ψ equal to 1. This correlation is presented in Section 7-4.3, Eqs. (7-125) through (7-152).

EXAMPLE 10-4

Pressure gradient calculation using the Beggs and Brill correlation

Calculate the pressure gradient for the flow of 2000 bbl/d oil and 1 MMSCF/d of gas described in Example 10-3.

Solution The first step in using this correlation is to determine the flow regime using Eqs. (7-131) through (7-134); however, we have already found the flow regime to be intermittent by using the flow regime map in Example 10-3. Note that the dashed lines in Fig. 10-4 correspond to Eqs. (7-131) through (7-134).

Next, we calculate the holdup for horizontal flow with Eq. (7-136). From Example 10-3, $\lambda_l = 0.35$ and $N_{\text{Fr}} = 17.8$, so

$$y_{lo} = \frac{(0.845)(0.35)^{0.5351}}{(17.8)^{0.0173}} = 0.458 \tag{10-23}$$

Even though there is no potential energy contribution to the pressure gradient in horizontal flow, the holdup is used as a parameter in calculating the frictional pressure gradient.

To calculate the frictional gradient, we first obtain the no-slip friction factor based on the mixture Reynolds number. Using Eqs. (7-143), (7-145), and (7-146),

$$\rho_m = (49.92)(0.35) + (2.6)(0.65) = 19.2 \text{ lb}_m/\text{ft}^3 \tag{10-24}$$

The Mandhane map (Fig. 10-3) is simply a plot of superficial liquid velocity versus superficial gas velocity. For our values of $u_{sl} = 3.81$ ft/sec and $u_{sg} = 7.11$ ft/sec, the flow regime is predicted to be slug flow.

The Beggs and Brill map plots the mixture Froude number, defined by Eq. (7-125), against the input fraction of liquid. These parameters are

$$N_{\text{Fr}} = \frac{(10.9 \text{ ft/sec})^2}{(32.17 \text{ ft/sec}^2)[(2.5/12) \text{ ft}]} = 17.8 \tag{10-21}$$

$$\lambda_l = \frac{3.81}{10.9} = 0.35 \tag{10-22}$$

From Fig. 10-4, the flow regime is predicted to be intermittent.

The prediction of dispersed bubble flow with the Baker map disagrees with that of Mandhane and Beggs and Brill, which predict slug flow. However, the conditions were very near the flow regime transition on the Baker map, and slug flow is the likely flow regime. ◇

Pressure gradient correlations. Over the years, numerous correlations have been developed to calculate the pressure gradient in horizontal gas-liquid flow. The most commonly used in the oil and gas industry today are those of Beggs and Brill (1973), Eaton et al. (1967), and Dukler (1969). These correlations all include a kinetic energy contribution to the pressure gradient; however, this can be considered negligible unless the gas rate is high and the pressure is low.

Beggs and Brill correlation. The Beggs and Brill correlation presented in Chapter 7 can be applied to horizontal flow, as well as flow in any other direction. For horizontal flow, the correlation is somewhat simplified, since the angle θ is 0, making the factor ψ equal to 1. This correlation is presented in Section 7-4.3, Eqs. (7-125) through (7-152).

EXAMPLE 10-4

Pressure gradient calculation using the Beggs and Brill correlation

Calculate the pressure gradient for the flow of 2000 bbl/d oil and 1 MMSCF/d of gas described in Example 10-3.

Solution The first step in using this correlation is to determine the flow regime using Eqs. (7-131) through (7-134); however, we have already found the flow regime to be intermittent by using the flow regime map in Example 10-3. Note that the dashed lines in Fig. 10-4 correspond to Eqs. (7-131) through (7-134).

Next, we calculate the holdup for horizontal flow with Eq. (7-136). From Example 10-3, $\lambda_l = 0.35$ and $N_{\text{Fr}} = 17.8$, so

$$y_{lo} = \frac{(0.845)(0.35)^{0.5351}}{(17.8)^{0.0173}} = 0.458 \tag{10-23}$$

Even though there is no potential energy contribution to the pressure gradient in horizontal flow, the holdup is used as a parameter in calculating the frictional pressure gradient.

To calculate the frictional gradient, we first obtain the no-slip friction factor based on the mixture Reynolds number. Using Eqs. (7-143), (7-145), and (7-146),

$$\rho_m = (49.92)(0.35) + (2.6)(0.65) = 19.2 \text{ lb}_m/\text{ft}^3 \tag{10-24}$$

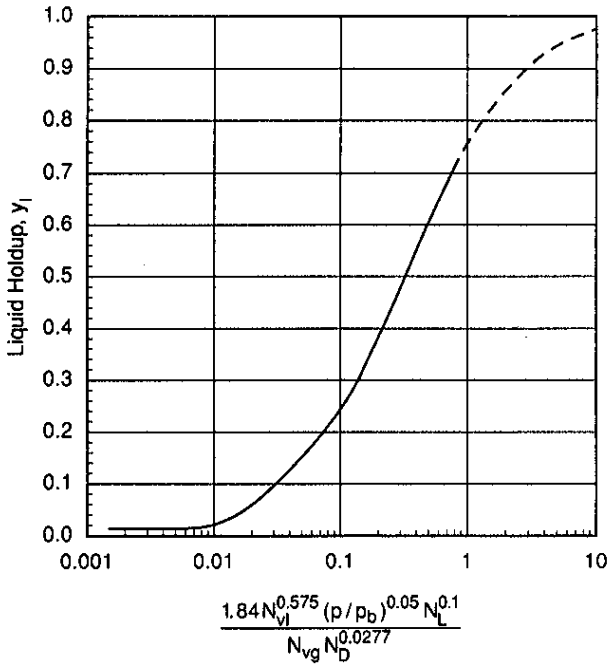

Figure 10-7
Eaton holdup correlation. (*From Eaton et al., 1966.*)

and reading from the correlation line for water in a 2-in. pipe (we choose this line because the pipe is closest to this size),

$$f\left(\frac{\dot{m}_l}{\dot{m}_m}\right)^{0.1} = 0.01 \tag{10-38}$$

so

$$f = \frac{0.01}{(6.5/7.13)^{0.1}} = 0.021 \tag{10-39}$$

Neglecting the kinetic energy term, the pressure gradient is given by Eq. (10-32),

$$\left(\frac{dp}{dx}\right)_F = \frac{(0.021)(19.16)(10.92)^2}{(2)(32.17)(2.5/12)} = 3.57 \text{ lb}_f/\text{ft}^3 = 0.025 \text{ psi/ft} \tag{10-40}$$

The liquid holdup is obtained from the correlation given by Fig. 10-7. The dimensionless numbers needed are given by Eqs. (7-99) through (7-102).

$$N_{vl} = (1.938)(3.81)\sqrt[4]{\frac{49.92}{30}} = 8.39 \tag{10-41}$$

$$N_{vg} = (1.98)(7.11)\sqrt[4]{\frac{49.92}{30}} = 15.65 \tag{10-42}$$

$$N_D = (120.872)\left(\frac{2.5}{12}\right)\sqrt{\frac{49.92}{30}} = 32.48 \tag{10-43}$$

$$N_L = (0.15726)(2)\sqrt[4]{\frac{1}{(49.92)(30)^3}} = 0.00923 \tag{10-44}$$

Calculating the abscissa value, we have

$$\frac{(1.84)N_{vl}^{0.575}(p/p_b)^{0.05}N_L^{0.1}}{N_{vg}N_D^{0.0277}} = \frac{(1.84)(8.39)^{0.575}(800/14.65)^{0.05}(0.00923)^{0.1}}{(15.65)(32.48)^{0.0277}} \tag{10-45}$$

$$= 0.277$$

and from Fig. 10-7, $y_l = 0.45$.

The liquid holdup predictions from the Beggs and Brill and Eaton correlations agree very closely; the Eaton correlation predicts a lower pressure gradient. ◇

Dukler correlation. The Dukler correlation (Dukler, 1969), like that of Eaton, is based on empirical correlations of friction factor and liquid holdup. The pressure gradient again consists of frictional and kinetic energy contributions:

$$\frac{dp}{dx} = \left(\frac{dp}{dx}\right)_F + \left(\frac{dp}{dx}\right)_{\text{KE}} \tag{10-46}$$

The frictional pressure drop is

$$\left(\frac{dp}{dx}\right)_F = \frac{f\rho_k u_m^2}{2g_c D} \tag{10-47}$$

where

$$\rho_k = \frac{\rho_l \lambda_l^2}{y_l} + \frac{\rho_g \lambda_g^2}{y_g} \tag{10-48}$$

Notice that the liquid holdup enters the frictional pressure drop through ρ_k. The friction factor is obtained from the no-slip friction factor, f_n, defined as

$$f_n = 0.0056 + 0.5(N_{\text{Re}_k})^{-0.32} \tag{10-49}$$

where the Reynolds number is

$$N_{\text{Re}_k} = \frac{\rho_k u_m D}{\mu_m} \tag{10-50}$$

The two-phase friction factor is given by the correlation

$$\frac{f}{f_n} = 1 - \frac{\ln \lambda_l}{1.281 + 0.478 \ln \lambda_l + 0.444(\ln \lambda_l)^2 + 0.094(\ln \lambda_l)^3 + 0.00843(\ln \lambda_l)^4} \tag{10-51}$$

The liquid holdup is given as a function of the input liquid fraction, λ_l, in Fig. 10-8, with N_{Re_k} as a parameter. Since the holdup is needed to calculate N_{Re_k} (ρ_k depends on y_l), determining the liquid holdup is an iterative procedure. We can begin by assuming that $y_l = \lambda_l$; an estimate of ρ_k and N_{Re_k} is then calculated. With these estimates, y_l is obtained from Fig. 10-8. We then compute new estimates of ρ_k and N_{Re_k}, repeating this procedure until convergence is achieved.

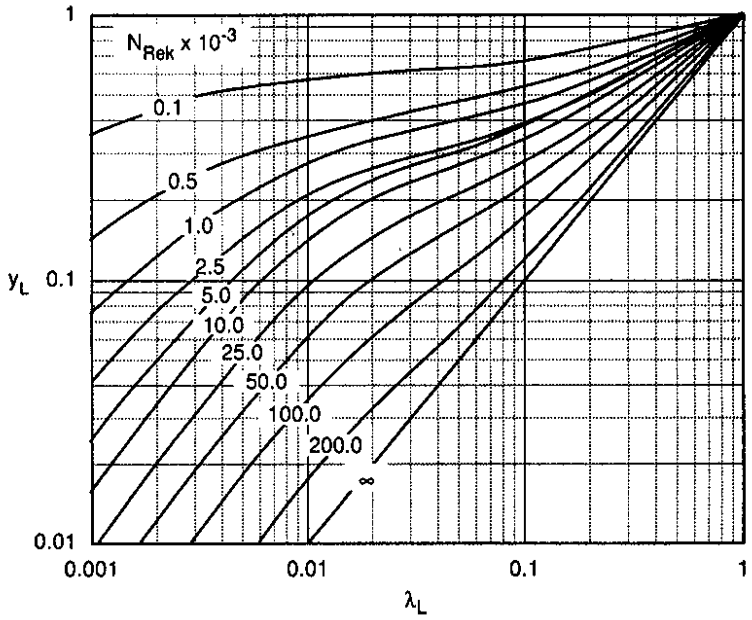

Figure 10-8
Dukler holdup correlation. (*From Dukler, 1969.*)

The pressure gradient due to kinetic energy changes is given by

$$\left(\frac{dp}{dx}\right)_{\mathrm{KE}} = \frac{1}{g_c\,\Delta x}\Delta\left(\frac{\rho_g u_{sg}^2}{y_g} + \frac{\rho_l u_{sl}^2}{y_l}\right) \tag{10-52}$$

EXAMPLE 10-6
Pressure gradient calculation using the Dukler correlation

Repeat Examples 10-4 and 10-5, using the Dukler correlation.

Solution An iterative procedure is required to find the liquid holdup. We begin by assuming that $y_l = \lambda_l$. In this case, $\rho_k = \rho_m$, found previously to be 19.16 $\mathrm{lb}_m/\mathrm{ft}^3$, and $N_{\mathrm{Re}_k} = N_{\mathrm{Re}_m}$, which was 91,600. From Fig. 10-8, we estimate y_l to be 0.44. Using this new value of liquid holdup,

$$\rho_k = \frac{(49.92)(0.35)^2}{0.44} + \frac{(2.6)(0.65)^2}{(1-0.44)} = 15.86\ \mathrm{lb}_m/\mathrm{ft}^3 \tag{10-53}$$

and

$$N_{\mathrm{Re}_k} = (91,600)\left(\frac{15.86}{19.16}\right) = 75{,}800 \tag{10-54}$$

Again reading y_l from Fig. 10-8, $y_l = 0.46$. This is the converged value.

The no-slip friction factor from Eq. (10-49) is

$$f_n = 0.0056 + (0.5)(75{,}800)^{-0.32} = 0.019 \tag{10-55}$$

From Eq. (10-51), we find

$$\frac{f}{f_n} = 1 - \frac{\ln(0.35)}{1.281 + 0.478[\ln(0.35)] + 0.444[\ln(0.35)]^2 + 0.094[\ln(0.35)]^3 + 0.00843[\ln(0.35)]^4}$$

$$= 1.90 \tag{10-56}$$

so

$$f = (1.90)(0.019) = 0.036 \tag{10-57}$$

Finally, from Eq. (10-47), we find the frictional pressure gradient to be

$$\left(\frac{dp}{dx}\right)_F = \frac{(0.036)(15.86)(10.92)^2}{(2)(32.17)(2.5/12)} = 5.08 \text{ lb}_f/\text{ft}^3 = 0.035 \text{ psi/ft} \tag{10-58}$$

We see that all three correlations predict essentially the same liquid holdup, but the pressure gradient predictions differ. ◇

Pressure traverse calculations. The correlations we have just examined provide a means of calculating the pressure gradient at a point along a pipeline; to determine the overall pressure drop over a finite length of pipe, the variation of the pressure gradient as the fluid properties change in response to the changing pressure must be considered. The simplest procedure is to evaluate fluid properties at the mean pressure over the distance of interest and then calculate a mean pressure gradient. For example, integrating the Dukler correlation over a distance L of pipe, we have

$$\Delta_P = \frac{\overline{f}\,\overline{\rho}_k \bar{u}_m^2 L}{2g_c D} + \frac{1}{g_c}\Delta\left(\frac{\rho_g u_{sg}^2}{y_g} + \frac{\rho_l u_{sl}^2}{y_l}\right) \tag{10-59}$$

The overbars indicate that f, ρ_k, and u_m are evaluated at the mean pressure, $(p_1 + p_2)/2$. In the kinetic energy term, the Δ means the difference between conditions at point 1 and point 2. If the overall pressure drop, $p_1 - p_2$, is known, the pipe length, L, can be calculated directly with this equation. When L is fixed, Δp must be estimated to calculate the mean pressure; using this mean pressure, Δp is calculated with Eq. (10-59), and, if necessary, the procedure is repeated until convergence is reached.

Since the overall pressure drop over the distance L is being calculated based on the mean properties over this distance, the pressure should not change too much over this

distance. In general, if the Δp over the distance L is greater than 10% of p_1, the distance L should be divided into smaller increments and the pressure drop over each increment calculated. The pressure drop over the distance L is then the sum of the pressure drops over the smaller increments.

EXAMPLE 10-7
Calculating the overall pressure drop

Just downstream from the wellhead choke, 2000 bbl/d of oil and 1 MM SCF/d of gas enters a 2.5-in. pipeline at 800 psia and 175°F (the same fluids as in the previous four examples). If these fluids are transported 3000 ft through this flow line to a separator, what is the discharge pressure at the separator? Use the Dukler correlation and neglect kinetic energy pressure losses.

Solution We found in Example 10-6 that the pressure gradient at the entrance conditions is 0.035 psi/ft. If this value holds over the entire line, the overall pressure drop would be (0.035)(3000) = 105 psi. Since this pressure drop is slightly greater than 10% of the entrance condition, we will divide the pipe into two length increments and calculate a mean pressure gradient over each increment.

It is most convenient to fix the Δp for the first increment and solve for the length of the increment. The remainder of the pipeline will then comprise the second section. We will choose a Δp of 60 psi for the first increment, L_1. Thus, for this section, $\bar{p} = 800 - 60/2 = 770$ psi. We previously calculated the properties of the fluids at 800 psi; the only property that may differ significantly at 770 psi is the gas density.

Following Example 4-3 for this gas, at 770 psi and 175°F, $p_{pr} = 1.07$ and $T_{pr} = 1.70$. From Fig. 4-1, $Z = 0.935$, and using Eq. (7-67),

$$\bar{\rho}_g = \frac{(28.97)(0.709)(770)}{(0.935)(10.73)(635)} = 2.5 \text{ lb}_m/\text{ft}^3 \tag{10-60}$$

The gas volumetric flow rate is then

$$\bar{q}_g = \frac{\dot{m}_g}{\bar{\rho}_g} = \frac{0.63 \text{ lb}_m/\text{sec}}{2.5 \text{ lb}_m/\text{ft}^3} = 0.252 \text{ ft}^3/\text{sec} \tag{10-61}$$

Since the liquid density is essentially the same at 770 psi as at the entrance condition, q_l is 0.13 ft^3/sec, as before, and the total volumetric flow rate is 0.252 + 0.13 = 0.382 ft^3/sec.

The input liquid fraction is 0.13/0.382 = 0.34, and the mixture velocity ($\bar{u}_m$) is found to be 11.2 ft/sec by dividing the total volumetric flow rate by the pipe cross-sectional area.

We can now use the Dukler correlation to calculate the pressure gradient at the mean pressure. We begin by estimating the liquid holdup at mean conditions to be the same as that found at the entrance, or $y_l = 0.46$. Then

$$\rho_k = \frac{(49.92 \text{ lb}_m/\text{ft}^3)(0.34)^2}{0.46} + \frac{(2.5 \text{ lb}_m/\text{ft}^3)(0.66)^2}{0.56} = 14.56 \text{ lb}_m/\text{ft}^3 \tag{10-62}$$

and

$$\mu_m = (2 \text{ cp})(0.34) + (0.0131 \text{ cp})(0.66) = 0.689 \text{ cp} \tag{10-63}$$

so,

$$N_{\text{Re}_k} = \frac{(14.56)(11.2)(2.5/12)}{(0.689)(6.72 \times 10^{-4})} = 73{,}400 \tag{10-64}$$

Checking Fig. 10-8, we find that $y_l = 0.46$, so no iteration is required. Using Eqs. (10-49) and (10-51), $f_n = 0.019$ and $f/f_n = 1.92$, so $f = 0.036$. From Eq. (10-47), we find that dp/dx is 0.034 psi/ft. The length of the first increment is

$$L_1 = \frac{\Delta p}{dp/dx} = \frac{60 \text{ psi}}{0.034 \text{ psi/ft}} = 1760 \text{ ft} \tag{10-65}$$

The remaining section of the pipeline is $3000 - 1760 = 1240$ ft long. If the pressure gradient over this section is also 0.034 psi/ft, the pressure drop will be 42 psi; thus we can estimate the mean pressure over the second increment to be $740 - 42/2 \approx 720$ psi.

With this mean pressure, we repeat the procedure to calculate the mean pressure gradient using the Dukler correlation and find that $dp/dx = 0.036$ psi/ft, giving an overall pressure drop for the second segment of 45 psi. Adding the two pressure drops, the pressure drop over the 3000-ft pipe is 105 psi. This happens to be exactly what we estimated using the pressure gradient at the pipe entrance conditions, illustrating that the pressure gradient is not varying significantly at these relatively high pressures. ◇

10-2.4 Pressure Drop through Pipe Fittings

When fluids pass through pipe fittings (tees, elbows, etc.) or valves, secondary flows and additional turbulence create pressure drops that must be included to determine the overall pressure drop in a piping network. The effects of valves and fittings are included by adding the "equivalent length" of the valves and fittings to the actual length of straight pipe when calculating the pressure drop. The equivalent lengths of many standard valves and fittings have been determined experimentally (Crane, 1957) and are given in Table 10-1. The equivalent lengths are given in pipe diameters; this value is multiplied by the pipe diameter to find the actual length of pipe to be added to account for the pressure drop through the valve or fitting.

10-3 Flow through Chokes

The flow rate from almost all flowing wells is controlled with a wellhead choke, a device that places a restriction in the flow line (Fig. 10-9.) A variety of factors may make it desirable to restrict the production rate from a flowing well, including the prevention of coning or sand production, satisfying production rate limits set by regulatory authorities, and meeting limitations of rate or pressure imposed by surface equipment.

When gas or gas-liquid mixtures flow through a choke, the fluid may be accelerated sufficiently to reach sonic velocity in the throat of the choke. When this condition occurs, the flow is called "critical," and changes in the pressure downstream of the choke do not affect the flow rate, because pressure disturbances cannot travel upstream faster than the sonic velocity. (Note: Critical flow is not related to the critical point of the fluid.) Thus, to predict the flow rate-pressure drop relationship for compressible fluids flowing through a choke, we must determine whether or not the flow is critical. Figure 10-10 shows the dependence of flow rate through a choke on the ratio of the downstream to upstream pressure for a compressible fluid, with the rate being independent of the pressure ratio when the flow is critical.

Table 10-1

Equivalent Lengths of Valves and Fittings[a]

Description of Fitting				Equivalent Length in Pipe Diameters
Globe valves	Stem perpendicular to run	With no obstruction in flat, bevel, or plug type seat	Fully open	340
		With wing or pin guided disk	Fully open	450
	Y-pattern	(No obstruction in flat, bevel, or plug type seat)		
		—With stem 60° from run of pipe line	Fully open	175
		—With step 45° from run of pipe line	Fully open	145
Angle valves		With no obstruction in flat, bevel, or plug type seat	Fully open	145
		With wing or pin-guided disk	Fully open	200
Gate valves	Wedge, disk		Fully open	13
	Double disk or plug disk		Three-quarters open	35
			One-half open	160
			One-quarter open	900
	Pulp stock		Fully open	17
			Three-quarters open	50
			One-half open	260
			One-quarter open	1200
Conduit pipe line gate, ball, and plug valves			Fully open	3
Check valves	Conventional swing		Fully open	135
	Clearway swing		Fully open	50
	Globe life or stop; stem perpendicular to run or Y-pattern		Fully open	Same as globe
	Angle lift or stop			Fully open
	Same as angle			
	In-line ball		Fully open	150

Table 10-1 (Continued)

Equivalent Lengths of Valves and Fittings[a]

		Description of Fitting		Equivalent Length in Pipe Diameters
Foot valves with strainer		With poppet lift-type disk	Fully open	420
		With leather-hinged disk	Fully open	75
Butterfly valves (8 in. and larger)			Fully open	40
Cocks	Straight-through	Rectangular plug port area equal to 100% of pipe area	Fully open	18
	Three-way	Rectangular plug port area equal to 80% of pipe area (fully open)	Flow straight through	44
			Flow through branch	140
Fittings	90° standard elbow			30
	45° standard elbow			16
	90° long radius elbow			20
	90° street elbow			50
	45° street elbow			26
	Square corner elbow			57
	Standard tee	With flow through run		20
		With flow through branch		60
	Close-pattern return bend			50

[a]From Crane (1957).

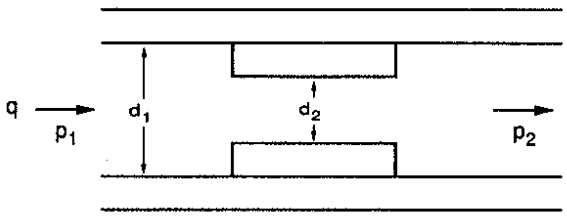

Figure 10-9
Choke schematic.

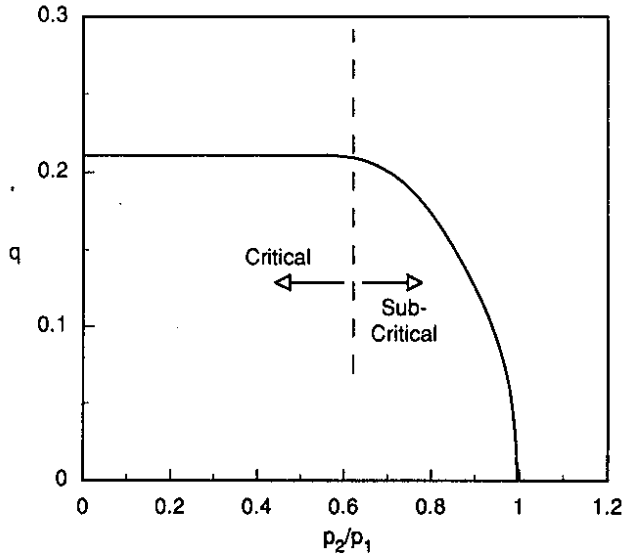

Figure 10-10
Dependence of flow rate through a choke on the ratio of the upstream to the downstream pressure.

In this section, we will examine the flow of liquid, gas, and gas-liquid mixtures through chokes.

10-3.1 Single-Phase Liquid Flow

The flow through a wellhead choke will rarely consist of single-phase liquid, since the flowing tubing pressure is almost always below the bubble point. However, when this does occur, the flow rate is related to the pressure drop across the choke by

$$q = CA\sqrt{\frac{2g_c\,\Delta p}{\rho}} \tag{10-66}$$

where C is the flow coefficient of the choke and A is the cross-sectional area of the choke. The flow coefficient for flow through nozzles is given in Fig. 10-11 (Crane, 1957) as a function of the Reynolds number in the choke and the ratio of the choke diameter to the pipe diameter. Equation (10-66) is derived by assuming that the pressure drop through the

choke is equal to the kinetic energy pressure drop divided by the square of a drag coefficient. This equation applies for subcritical flow, which will usually be the case for single-phase liquid flow.

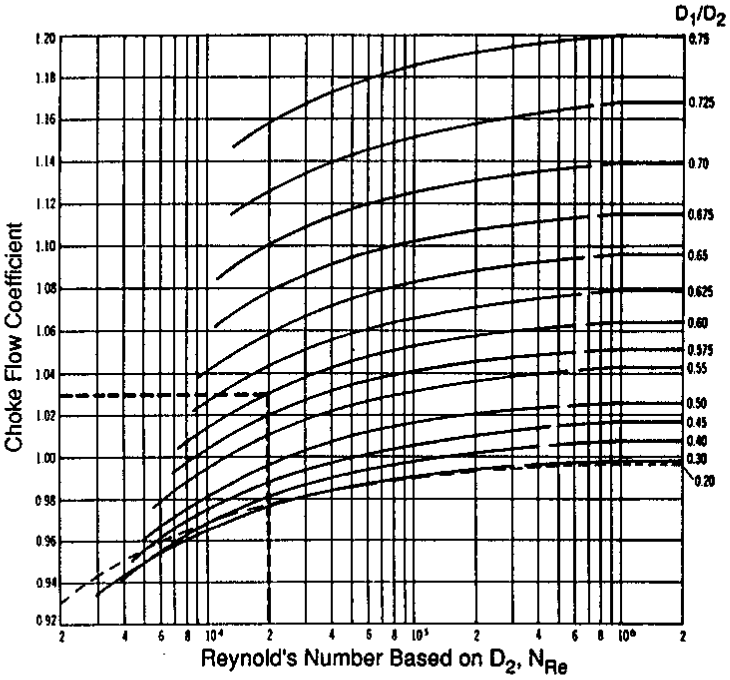

Figure 10-11
Flow coefficient for liquid flow through a choke. (*From Crane, 1957.*)

For oilfield units, Eq. (10-66) becomes

$$q = 22{,}800C(D_2)^2\sqrt{\frac{\Delta p}{\rho}} \tag{10-67}$$

where q is in bbl/d, D_2 is the choke diameter in in., Δp is in psi, and ρ is in lb_m/ft^3. The choke diameter is often referred to as the "bean size," because the device in the choke that restricts the flow is called the bean. Bean sizes are usually given in 64ths of an inch.

EXAMPLE 10-8
Liquid flow through a choke

What will be the flow rate of a 0.8-specific gravity, 2-cp oil through a 20/64-in. choke if the pressure drop across the choke is 20 psi and the line size in 1 in.?

Solution Figure 10-11 gives the flow coefficient as a function of the diameter ratio and the Reynolds number through the choke. Since we do not know the Reynolds number until we know the flow rate, we assume that the Reynolds number is high enough that the flow coefficient is independent of Reynolds number. For $D_2/D_1 = 0.31$, C is approximately 1.00. Then, from

Eq. (10-67),

$$q = (22{,}800)(1.00)\left(\frac{20}{64}\right)^2\sqrt{\frac{20}{49.92}} = 1410 \text{ bbl/d} \tag{10-68}$$

Checking the Reynolds number through the choke [Eq. (7-7)], we find $N_{Re} = 1.67 \times 10^5$. From Fig. 10-11, $C = 0.99$ for this N_{Re}; using this value, the flow rate is 1400 bbl/d. ◇

10-3.2 Single-Phase Gas Flow

When a compressible fluid passes through a restriction, the expansion of the fluid is an important factor. For isentropic flow of an ideal gas through a choke, the rate is related to the pressure ratio, p_2/p_1, by (Szilas, 1975)

$$q_g = \frac{\pi}{4}D_2^2 p_1 \frac{T_{sc}}{p_{sc}}\alpha\sqrt{\left(\frac{2g_c R}{28.97\gamma_g T_1}\right)\left(\frac{\gamma}{\gamma-1}\right)\left[\left(\frac{p_2}{p_1}\right)^{2/\gamma} - \left(\frac{p_2}{p_1}\right)^{(\gamma+1)/\gamma}\right]} \tag{10-69}$$

which can be expressed in oilfield units as

$$q_g = 3.505 D_{64}^2\left(\frac{p_1}{p_{sc}}\right)\alpha\sqrt{\left(\frac{1}{\gamma_g T_1}\right)\left(\frac{\gamma}{\gamma-1}\right)\left[\left(\frac{p_2}{p_1}\right)^{2/\gamma} - \left(\frac{p_2}{p_1}\right)^{(\gamma+1)/\gamma}\right]} \tag{10-70}$$

where q_g is in MSCF/d, D_{64} is the choke diameter (bean size) in 64ths of inches (e.g., for a choke diameter of 1/4 in., $D_2 = 16/64$ in. and $D_{64} = 16$), T_1 is the temperature upstream of the choke in °R, γ is the heat capacity ratio, C_p/C_v, α is the flow coefficient of the choke, γ_g is the gas gravity, p_{sc} is standard pressure, and p_1 and p_2 are the pressures upstream and downstream of the choke, respectively.

Equations (10-69) and (10-70) apply when the pressure ratio is equal to or greater than the critical pressure ratio, given by

$$\left(\frac{p_2}{p_1}\right)_c = \left(\frac{2}{\gamma+1}\right)^{\gamma/(\gamma-1)} \tag{10-71}$$

When the pressure ratio is less than the critical pressure ratio, p_2/p_1 should be set to $(p_2/p_1)c$ and Eq. (10-70) used, since the flow rate is insensitive to the downstream pressure whenever the flow is critical. For air and other diatomic gases, γ is approximately 1.4, and the critical pressure ratio is 0.53; in petroleum engineering operations, it is commonly assumed that flow through a choke is critical whenever the downstream pressure is less than about half of the upstream pressure.

EXAMPLE 10-9

The effect of choke size on gas flow rate

Construct a chart of gas flow rate versus pressure ratio for choke diameters (bean sizes) of 8/64, 12/64, 16/24, 20/64, and 24/64 of an inch. Assume that the choke flow coefficient is 0.85, the gas gravity is 0.7, γ is 1.25, and the wellhead temperature and flowing pressure are 100°F and 600 psia.

Solution From Eq. (10-71), we find that the critical pressure ratio is 0.56 for this gas. Using Eq. (10-70),

$$q_g = 3.505 D_{64}^2 \left(\frac{600}{14.7}\right)(0.85)\sqrt{\left(\frac{1}{(0.7)(560)}\right)\left(\frac{1.25}{1.25-1}\right)\left[\left(\frac{p_2}{p_1}\right)^{2/1.25} - \left(\frac{p_2}{p_1}\right)^{(1.25+1)/1.25}\right]} \tag{10-72}$$

or

$$q_g = 13.73 D_{64}^2 \sqrt{\left(\frac{p_2}{p_1}\right)^{1.6} - \left(\frac{p_2}{p_1}\right)^{1.8}} \tag{10-73}$$

The maximum gas flow rate will occur when the flow is critical, that is, when $(p_2/p_1) = 0.56$. For any value of the pressure ratio below the critical value, the flow rate will be the critical flow rate. Using values of p_2/p_1 from 0.56 to 1 for each choke size, Fig. 10-12 is constructed. ◇

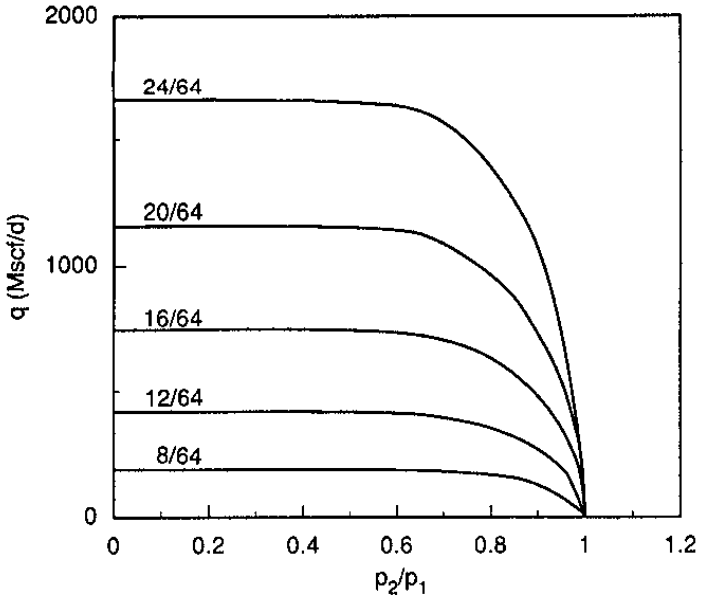

Figure 10-12
Gas flow performance for different choke sizes.

10-3.3 Gas-Liquid Flow

Two-phase flow through a choke has not been described well theoretically. To determine the flow rate of two phases through a choke, empirical correlations for critical flow are generally used. Some of these correlations are claimed to be valid up to pressure ratios of 0.7 (Gilbert, 1954). One means of estimating the conditions for critical two-phase flow through a choke is to compare the velocity in the choke with the two-phase sonic velocity, given by Wallis (1969) for homogeneous mixtures as

$$v_c = \left\{\left[\lambda_g \rho_g + \lambda_l \rho_l\right]\left[\frac{\lambda_g}{\rho_g v_{gc}^2} + \frac{\lambda_l}{\rho_l v_{lc}^2}\right]\right\}^{-1/2} \tag{10-74}$$

where v_c is the sonic velocity of the two-phase mixture and v_{gc} and v_{lc} are the sonic velocities of the gas and liquid, respectively.

The empirical correlations of Gilbert (1954) and Ros (1960) have the same form, namely,

$$p_1 = \frac{Aq_l(\text{GLR})^B}{D_{64}^C} \tag{10-75}$$

differing only in the empirical constants A, B, and C, given in Table 10-2. The upstream pressure, p_1, is in psig in the Gilbert correlation and psia in Ros's correlation. In these correlations, q_l is the liquid rate in bbl/d, GLR is the producing gas–liquid ratio in SCF/bbl, and D_{64} is the choke diameter in 64ths of an inch.

Table 10-2

Empirical Constants in Two-Phase Critical Flow Correlations

Correlation	A	B	C
Gilbert	10.00	0.546	1.89
Ros	17.40	0.500	2.00

Another empirical correlation that may be preferable for certain ranges of conditions is that of Omana et al. (1969). Based on dimensional analysis and a series of tests with natural gas and water, the correlation is

$$N_{ql} = 0.263 N_\rho^{-3.49} N_{pl}^{3.19} \lambda_l^{0.657} N_D^{1.80} \tag{10-76}$$

with dimensionless groups defined as

$$N_\rho = \frac{\rho_g}{\rho_l} \tag{10-77}$$

$$N_{p1} = 1.74 \times 10^{-2} p_1 \left(\frac{1}{\rho_l \sigma_l}\right)^{0.5} \tag{10-78}$$

$$N_D = 0.1574 D_{64} \sqrt{\frac{\rho_l}{\sigma_l}} \tag{10-79}$$

$$N_{ql} = 1.84 q_l \left(\frac{\rho_l}{\sigma_l}\right)^{1.25} \tag{10-80}$$

For the constants given, the oilfield units are q, bbl/d; ρ, lb_m/ft^3; σ_l, dyhes/cm; D_{64}, 64ths of an inch; and p_1, psia. The Omana correlation is restricted to critical flow, requiring that $q_g/q_l > 1.0$ and $p_2/p_1 < 0.546$. It is best suited to low-viscosity liquids (near the viscosity of water) and choke diameters (bean sizes) of 14/64 in. or less. The fluid properties are evaluated at the upstream conditions.

EXAMPLE 10-10
Finding the choke size for gas-liquid flow

For the flow of 2000 bbl/d of oil and 1 MMSCF/d of gas at a flowing tubing pressure of 800 psia as described in Example 10-3, find the choke diameter (bean size) using the Gilbert, Ros, and Omana correlations.

Solution For the Gilbert and Ros correlations, solving Eq. (10-75) for the choke diameter, we have

$$D_{64} = \left(\frac{Aq_l(\text{GLR})^B}{p_1}\right)^{1/C} \tag{10-81}$$

For the given flow rate of 2000 bbl/d, a GLR of 500 SCF/bbl, and an absolute pressure of 800 psi upstream of the choke, from the Gilbert correlation,

$$D_{64} = \left(\frac{(10)(2000)(500)^{0.546)}}{800 - 14.7}\right)^{1/1.89} = 33 \text{ 64ths of an inch} \tag{10-82}$$

and, from the Ros correlation,

$$D_{64} = \left(\frac{(17.4)(2000)(500)^{0.5}}{800}\right)^{0.5} = 31 \text{ 64ths of an inch} \tag{10-83}$$

With the Omana correlation, we solve Eq. (10-76) for N_D:

$$N_D = \left(\frac{1}{0.263} N_{qi} N_\rho^{3.49} N_{p_1}^{-3.19} \lambda_l^{-0.657}\right)^{1/1.8} \tag{10-84}$$

From Example 10-3, $\lambda_l = 0.35$, $\rho_l = 49.92$ lb$_m$/ft^3, $\rho_g = 2.6$ lb$_m$/ft^3, and $\sigma_l = 30$ dynes/cm. From Eqs. (10-77), (10-78), and (10-80),

$$N_\rho = \frac{2.6}{49.92} = 0.0521 \tag{10-85}$$

$$N_{p1} = (1.74 \times 10^{-2})(800)\left[\frac{1}{(49.92)(30)}\right]^{0.5} = 0.36 \tag{10-86}$$

$$N_{ql} = (1.84)(2000)\left(\frac{49.92}{30}\right)^{1.25} = 6.95 \times 10^3 \tag{10-87}$$

Then

$$N_D = \left[\left(\frac{1}{0.263}\right)(6.95 \times 10^3)(0.0521)^{3.49}(0.36)^{-3.19}(0.35)^{-0.657}\right]^{1/1.8} = 8.35 \tag{10-88}$$

Solving Eq. (10-79) for the choke diameter, we have

$$D_{64} = \frac{N_D}{(0.1574)\sqrt{\frac{\rho_l}{\sigma_l}}} \tag{10-89}$$

so

$$D_{64} = \frac{8.35}{(0.1574)\sqrt{49.92/30}} = 41 \text{ 64ths of an inch} \tag{10-90}$$

The Gilbert and Ros correlations predict a choke size of about 1/2 in. (32/64 in.), while the Omana correlation predicts a larger choke size of 41/64 in. Since the Omana correlation was based on liquid flow rates of 800 bbl/d or less, the Gilbert and Ros correlations are probably the more accurate in this case. ◇

When a well is being produced with critical flow through a choke, the relationship between the wellhead pressure and the flow rate is controlled by the choke, since downstream pressure disturbances (such as a change in separator pressure) do not affect the flow performance through the choke. Thus, the attainable flow rate from a well for a given choke can be determined by matching the choke performance with the well performance, as determined by a combination of the well IPR and the vertical lift performance. The choke performance curve is a plot of the flowing tubing pressure versus the liquid flow rate, and can be obtained from the two-phase choke correlations, assuming that the flow is critical.

EXAMPLE 10-11
Choke performance curves

Construct performance curves for 16/64-, 24/64-, and 32/64-in. chokes for a well with a GLR of 500, using the Gilbert correlation.

Solution The Gilbert correlation predicts that the flowing tubing pressure is a linear function of the liquid flow rate, with an intercept at the origin. Using Eq. (10-75), we find

$$p_{tf} = 1.57 q_l \quad \text{for 16/64-in. choke} \tag{10-91}$$

$$p_{tf} = 0.73 q_l \quad \text{for 24/64-in. choke} \tag{10-92}$$

$$p_{tf} = 0.43 q_l \quad \text{for 32/64-in. choke} \tag{10-93}$$

These relationships are plotted in Fig. 10-13, along with a well performance curve. The intersections of the choke performance curves with the well performance curve are the flow rates that would occur with these choke sizes. Note that the choke correlation is valid only when the flow through the choke is critical; for each choke, there will be a flow rate below which flow through the choke is subcritical. This region is indicated by the dashed portions of the choke performance curves—the predictions are not valid for these conditions. ◇

10-4 SURFACE GATHERING SYSTEMS

In most oil and gas production installations, the flow from several wells will be gathered at a central processing station or combined into a common pipeline. Two common types of gathering systems were illustrated by Szilas (1975) (Fig. 10-14). When the individual well flow rates are controlled by critical flow through a choke, there is little interaction among the wells. However, when flow is subcritical, the downstream pressure can influence the performance of the wells, and the flow through the entire piping network may have to be treated as a system.

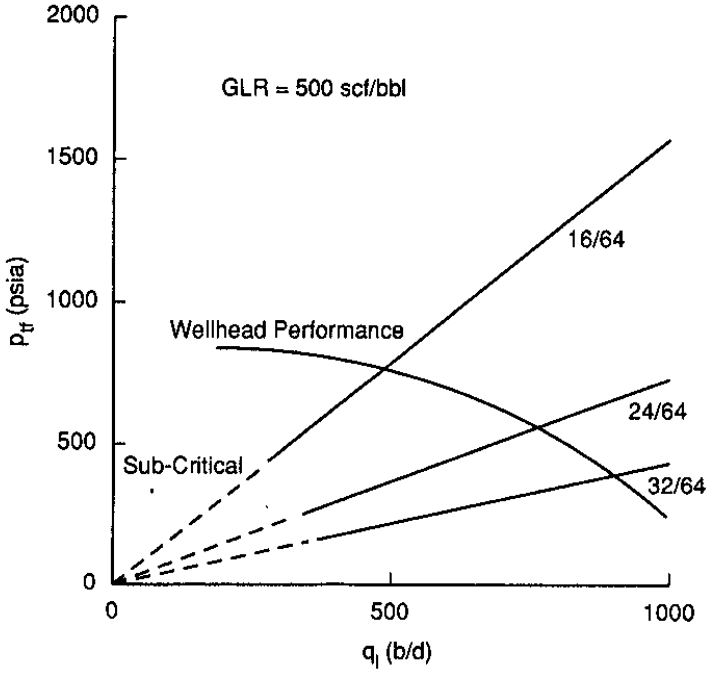

Figure 10-13
Choke performance curves (Example 10-11).

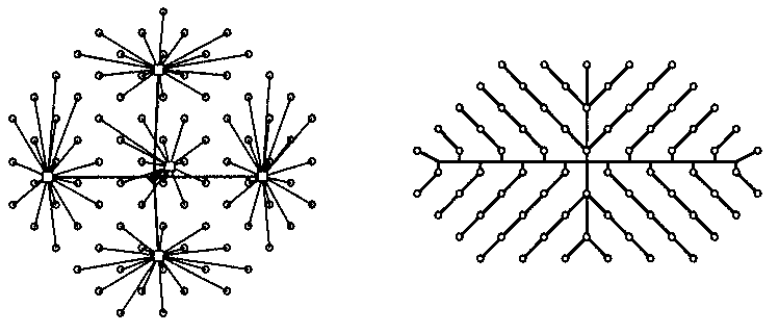

Figure 10-14
Oil and gas production gathering systems. (*From Szilas, 1975.*)

When individual flow lines all join at a common point (Fig. 10-14, left), the pressure at the common point is equal for all flow lines. The common point is typically a separator in an oil production system. The flowing tubing pressure of an individual well i is related to the separator pressure by

$$ptfi = p_{sep} + \Delta p_{Li} + \Delta p_{Ci} + \Delta p_{fi} \tag{10-94}$$

where Δp_{Li} is the pressure drop through the flow line, Δp_{Ci} is the pressure drop through the choke (if present), and Δp_{fi} is the pressure drop through fittings.

In a gathering system where individual wells are tied into a common pipeline, so that the pipeline flow rate is the sum of the upstream well flow rates as in Fig. 10-14, right, each

well has a more direct effect on its neighbors. In this type of system, individual wellhead pressures can be calculated by starting at the separator and working upstream.

Depending on the lift mechanism of the wells, the flow rates of the individual wells may depend on the flowing tubing pressures. In this case, the IPRs and vertical lift performance characteristics of the wells and surface gathering system must all be considered together to predict the performance of the well network. This will be treated in Chapter 21.

EXAMPLE 10-12

Analysis of a surface gathering system

The liquid production from three rod-pumped wells is gathered in a common 2-in. line, as shown in Fig. 10-15. One-inch flow lines connect each well to the gathering line, and each well line contains a ball valve and a conventional swing check valve. Well 1 is tied into the gathering line with a standard 90° elbow, while wells 2 and 3 are connected with standard tees. The oil density is 0.85 g/cm^3 (53.04 lb$_m$/ft^3), and its viscosity is 5 cp. The separator pressure is 100 psig. Assuming the relative roughness of all lines to be 0.001, calculate the flowing tubing pressures of the three wells.

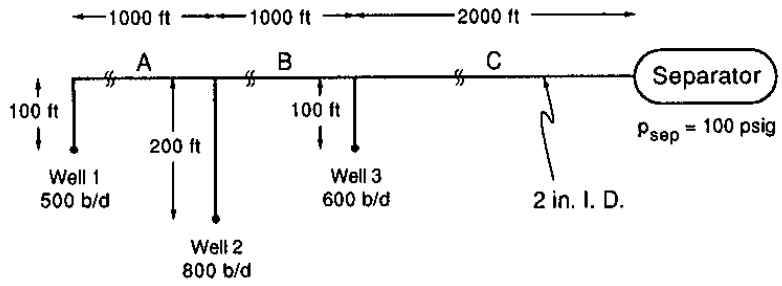

Figure 10-15

Surface gathering system (Example 10-12).

Solution Since the flow rates are all known (and are assumed independent of the wellhead pressures for these rod-pumped wells), the pressure drop for each pipe segment can be calculated independently using Eq. (10-1). The friction factors are obtained from the Chen equation [Eq. (7-35)] or the Moody diagram (Fig. 7-7). The pressure drops through the fittings and valves in the well flow lines are considered by adding their equivalent lengths from Table 10-1 to the well flow line lengths. For example, for well flow line 2, the ball valve adds 3 pipe diameters, the check valve 135 pipe diameters, and the tee (with flow through a branch) 60 pipe diameters. The equivalent length of flow line 2 is then (3 + 135 + 60)(1/12 ft) + 200 ft = 216.5 ft. A summary of the calculated results are given in Table 10-3.

The pressure at each point in the pipe network is obtained by starting with the known separator pressure and adding the appropriate pressure drops. The resulting system pressures are shown in Fig. 10-16. The differences in the flowing tubing pressures in these wells would result in different fluid levels in the annuli, if the IPRs and elevations are the same in all three wells. ◇

Table 10-3

Pressure Drop Calculation Results

Gathering Line

Segment	q (bbl/d)	N_{Re}	f	u (ft/sec)	Δp (psi)
A	500	3,930	0.0103	1.49	3
B	1,300	10,200	0.0081	3.88	17
C	1,900	14,900	0.0077	5.66	68

Well Flow Lines

Well No.	N_{Re}	f	u (ft/sec)	$(L/D)_{fittings}$	L (ft)	Δp (psi)
1	7,850	0.0086	5.96	168	114	10
2	12,600	0.0077	9.54	198	216.5	42
3	9,420	0.0082	7.16	198	116.5	13

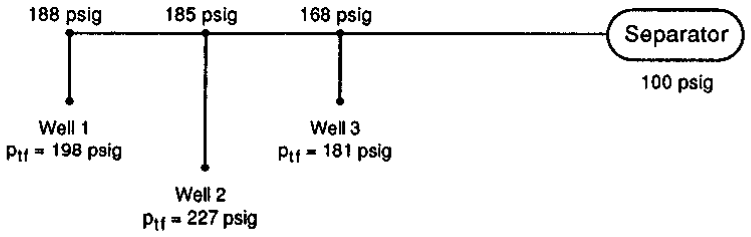

Figure 10-16
Pressure distribution in gathering system (Example 10-12).

REFERENCES

1. Baker, O., "Design of Pipelines for the Simultaneous Flow of Oil and Gas," *Oil and Gas J.*, **53**: 185, 1953.
2. Beggs, H. D., and Brill, J. P., "A Study of Two-Phase Flow in Inclined Pipes," *JPT*, 607–617, May 1973.
3. Brill, J. P., and Beggs, H. D., *Two-Phase Flow in Pipes*, University of Tulsa, Tulsa, OK, 1978.
4. Crane Co., "Flow of Fluids through Valves, Fittings, and Pipe," Technical Paper No. 410, Chicago, 1957.
5. Dukler, A. E., "Gas-Liquid Flow in Pipelines," American Gas Association, American Petroleum Institute, Vol. 1, *Research Results*, May 1969.
6. Eaton, B. A., Andrews, D. E., Knowles, C. E., and Silberberg, I. H., and Brown, K. E., "The Prediction of Flow Patterns, Liquid Holdup, and Pressure Losses Occurring during Continuous Two-Phase Flow in Horizontal Pipelines, *Trans. AIME*, **240**: 815–828, 1967.
7. Gilbert, W. E., "Flowing and Gas-Lift Well Performance," *API Drilling and Production Practice*, p. 143, 1954.
8. Mandhane, J. M., Gregory, G. A., and Aziz, K., "A Flow Pattern Map for Gas-Liquid Flow in Horizontal Pipes," *Int. J. Multiphase Flow*, **1**: 537–553, 1974.

9. Omana, R., Houssiere, C., Jr., Brown, K. E., Brill, J. P., and Thompson, R. E., "Multiphase Flow through Chokes", SPE Paper 2682, 1969.
10. Ros, N. C. J., "An Analysis of Critical Simultaneous Gas/Liquid Flow through a Restriction and Its Application to Flowmetering," *Appl. Sci. Res.*, **9**, Sec. A, p. 374, 1960.
11. Scott, D. S., "Properties of Cocurrent Gas-Liquid Flow," *Advances in Chemical Engineering, Volume 4*, Drew, T. B., Hoopes, J. W., Jr., and Vermeulen, T., eds., Academic Press, New York, pp. 200–278, 1963.
12. Szilas, A. P., *Production and Transport of Oil and Gas*, Elsevier, Amsterdam, 1975.
13. Taitel, Y., and Dukler, A. E., "A Model for Predicting Flow Regime Transitions in Horizontal and Near Horizontal Gas-Liquid Flow," *AICHE J.*, **22** (1): 47–55, January 1976.
14. Wallis, G. B., *One Dimensional Two-Phase Flow*, McGraw-Hill, New York, 1969.

PROBLEMS

10-1. Suppose that 3000 bbl/d of injection water is supplied to a well by a central pumping station located 2000 ft away, where the pressure is 400 psig. The water has a specific gravity of 1.02 and a viscosity of 1 cp. Determine the smallest diameter flow line (within the nearest 1/2 in.) that can be used to maintain a wellhead pressure of at least 300 psig if the pipe relative roughness is 0.001.

10-2. Suppose that 2 MMSCF/d of natural gas with specific gravity of 0.7 is connected to a pipeline with 4000 ft of 2-in. flow line. The pipeline pressure is 200 psig and the gas temperature is 150°F. Calculate the wellhead pressure assuming: (a) smooth pipe; (b) $\epsilon = 0.001$.

10-3. A 20/64-in. choke ($\alpha = 0.9$) is added to the flowline of Problem 10-2. Repeat the calculations of wellhead pressure.

10-4. Using the Baker, Mandhane, and Beggs and Brill flow regime maps, find the flow regime for the flow of 500 bbl/d oil and 1000 SCF/bbl of associated gas in a 2-in. flow line. The oil and gas are those described in Appendix B, $\sigma_l = 20$ dynes/cm, the temperature is 120°F, and the pressure is 1000 psia.

10-5. Repeat Problem 10-4, but for a pressure of 100 psia.

10-6. Using the Beggs and Brill, Eaton, and Dukler correlations, calculate the pressure gradient for the flow of 4000 bbl/d of oil and 500 SCF/bbl of associated gas (Appendix B oil and gas) flowing in a 3-in.-I.D. line with a relative roughness of 0.001. $T = 150$°F, $p = 200$ psia, and $\sigma_l = 20$ dynes/cm. Neglect the kinetic energy pressure gradient.

10-7. Repeat Problem 10-6 for 1000 bbl/d oil, GOR = 1000, $p = 400$ psia, in a 1 1/2-in. flow line.

10-8. Repeat Problem 10-6 for 2000 bbl/d, GOR = 1000, $p = 100$ psia in a 2-in. flow line.

10-9. For the flow described in Problem 10-6, assume that the pressure given is the wellhead pressure. What is the maximum possible length of this flow line?

10-10. Construct choke performance curves for flowing tubing pressures up to 1000 psi for the well of Appendix A for choke sizes of 8/64, 12/64, and 16/64 in.

10-11. Construct choke performance curves for flowing tubing pressures up to 1000 psi for the well of Appendix B for choke sizes of 8/64, 12/64, and 16/64 in.

10-12. Construct choke performance curves for flowing tubing pressures up to 1000 psi for the gas well of Appendix C for choke sizes of 8/64, 12/64, and 16/64 in.

10-13. The liquid production from several rod-pumped wells producing from the reservoir of Appendix A are connected to a separator with the piping network shown in Fig. 10-17. The relative roughness of all pipes is 0.001. For a separator pressure of 150 psig and assuming that the temperature is approximately 100°F throughout the system, find the wellhead pressures of the wells.

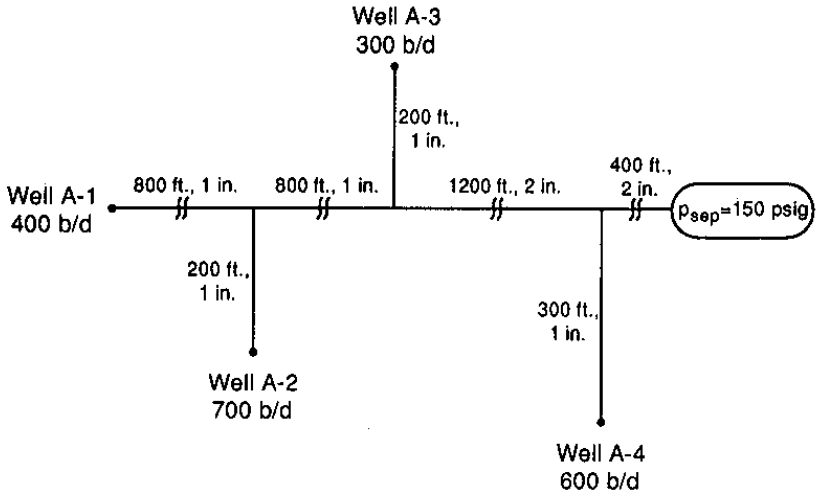

Figure 10-17
Surface gathering system (Problem 10-13).

10-14. Redesign the piping network of Problem 10-13 so that no wellhead pressure is greater than 225 psig by changing the pipe diameters of as few pipe segments as possible.